Applied Geochemistry 171 (2024) 106091

Contents lists available at ScienceDirect

Applied Geochemistry

journal homepage: www.elsevier.com/locate/apgeochem

Thermodynamic description of U(IV) solubility and hydrolysis in chloride systems: Pitzer activity model for the system U^{4+}–Na^{+}–Mg^{2+}–Ca^{2+}–H^{+}–Cl^{-}–OH^{-}–$H_2O(l)$

Y. Yan [**], N. Çevirim-Papaioannou, X. Gaona [*], D. Fellhauer, M. Altmaier

Karlsruhe Institute of Technology, Institute for Nuclear Waste Disposal, Karlsruhe, Germany

ARTICLE INFO

Editorial handling by: Dr Mavrik Zavarin

Keywords:
Uranium
Solubility
Hydrolysis
Thermodynamics
Pitzer

ABSTRACT

This study presents updated chemical, thermodynamic, and activity models for the system U^{4+}–Na^{+}–Mg^{2+}–Ca^{2+}–H^{+}–Cl^{-}–OH^{-}–$H_2O(l)$ derived using the Pitzer formalism and a strict ion interaction approach. The models build on comprehensive solubility datasets in dilute to concentrated NaCl, $MgCl_2$, and $CaCl_2$ solutions. The Nuclear Energy Agency-Thermochemical Database (NEA-TDB) selection of solubility and hydrolysis constants in the reference state were taken as anchoring point, and were extended further with the solid nanocrystalline phase $UO_2{\bullet}H_2O(ncr)$ and the ternary complex $Ca_4[U(OH)_8]^{4+}$. The former was identified in long-term solubility experiments at ambient conditions, whereas the latter has been selected in analogy to Th(IV), Np(IV), and Pu(IV) considering experimental evidences available for these An(IV) in alkaline, concentrated $CaCl_2$ solutions. These models represent an improved tool for the calculation of U(IV) solubility and aqueous speciation in a variety of geochemical conditions including concentrated brine systems relevant in salt-based repositories for nuclear waste disposal.

1. Introduction

Uranium is a relevant actinide for the long-term safety assessment of deep geological repositories for the disposal of nuclear waste due to its large inventory in spent nuclear fuel and the long half-lives of U isotopes in the waste, mostly ^{238}U ($t_{1/2} = 4.468{\bullet}10^9$ a), but also ^{235}U ($t_{1/2} = 7.04{\bullet}10^8$ a) and ^{236}U ($t_{1/2} = 2.342{\bullet}10^7$ a). Under the reducing conditions foreseen after repository closure, uranium is predominantly expected in its + IV oxidation state. Because of its high charge-to-size ratio (z/d), U(IV) is characterized by a strong hydrolysis and the formation of sparingly soluble hydrous oxides (Altmaier et al., 2013; Grenthe et al., 2020; Neck et al., 1992). Solubility data available for U(IV) (and for tetravalent actinides in general) are often characterized by a large dispersion, which reflects differences in the solid phase stability. The latter can be rationalized in terms of differences in particle size, degree of crystallinity, or number of hydration waters. As other tetravalent actinides (e.g., Pu and Np, and to a lesser extent Th), U(IV) hydrolyzes already at very low pH values, which hinders the possibility of directly studying the principal solubility equilibrium between $UO_2(s)$ and the unhydrolyzed aquo ion U^{4+} experimentally. This imposes a correlation between the solubility product of the given $UO_2(s)$ solid phase/s and the hydrolysis scheme considered for the description of the aqueous speciation.

Predictions of the chemical behavior of U(IV) under repository-relevant conditions rely on the availability of complete and accurate chemical and thermodynamic models. In the case of repositories in salt-rock formations, the boundary conditions may potentially include saturated NaCl and $MgCl_2$ brines with salt concentrations ≈5 mol/L and ≈4.5 mol/L, respectively. Intermediate ionic strength conditions ($2 < I < 6$ mol/L) are also expected in specific clay formations such as Cretaceous argillites in Northern Germany (Brewitz, 1980) or sedimentary bedrocks in the Canadian Shield (Frape et al., 1984), among other examples.

A number of experimental and theoretical studies providing solubility and hydrolysis constants (corresponding to either $U^{4+} + nH_2O(l) \rightleftharpoons U(OH)_n^{4-n} + nH^+$ or $U^{4+} + nOH^- \rightleftharpoons U(OH)_n^{4-n}$) for U(IV) are available in the literature (Bruno et al., 1986; Galkin and Stepanov, 1961; Gayer and Leider, 1957; Kraus and Nelson, 1950; Neck and Kim, 2001; Parks and Pohl, 1988; Rai et al., 1990, 1997; Ryan and Rai, 1983; Tremaine et al., 1981; Yajima et al., 1994), and were critically reviewed in the 1st

---

[*] Corresponding author.

[**] Corresponding author.

E-mail addresses: yiru.yan@ri.se (Y. Yan), xavier.gaona@kit.edu (X. Gaona).

https://doi.org/10.1016/j.apgeochem.2024.106091
Received 29 March 2024; Received in revised form 19 June 2024; Accepted 30 June 2024

(Grenthe et al., 1992) and 5th (Guillaumont et al., 2003) volumes of the Nuclear Energy Agency-Thermochemical Database (NEA-TDB) project. Since then, some newer studies investigated the solubility and hydrolysis of U(IV) using different techniques, including solvent extraction (Fujiwara et al., 2003), solubility measurements (Cevirim-Papaioannou, 2018; Fujiwara et al., 2005; Rai et al., 2003), electromotive force (emf) measurements (Manfredi et al., 2006), and coulometric titrations (Opel et al., 2007). Activity models were provided in some of these studies, mostly accounting for the Specific Ion Interaction Theory (SIT) (Ciavatta, 1980). Based on the NEA-TDB selection for U(IV) solubility and hydrolysis constants as well as data available at high chloride concentrations and the use of estimation methods, Neck and co-workers provided a complete set of Pitzer parameters for the modeling of activity coefficients for U^{4+}, UOH^{3+}, $U(OH)_2^{2+}$, and $U(OH)_3^+$ in chloride medium (Neck et al., 2001). This selection was later implemented in the German Thermodynamic Reference Database (THEREDA, www.thereda.de) (Moog et al., 2015; Fujiwara et al., 2003) combined solubility and solvent extraction studies to derive the thermodynamic properties of U(IV) hydrolysis species. Oversaturation experiments revealed an increase of the solubility with pH in hyperalkaline systems, which was attributed to the formation of the anionic U(IV) species $U(OH)_5^-$ and $U(OH)_6^{2-}$. This hypothesis was later refuted by (Çevirim-Papaioannou et al., 2018), who demonstrated that the enhanced U concentrations are caused by the slow reduction kinetics of U(VI) in oversaturation experiments. (Rai et al., 2003) conducted an accurate solubility study using UO_2(cr) precipitated from U(IV) at 90 °C at different pH values. While the initial crystalline phase, UO_2(cr), was found to control the U(IV) solubility in systems precipitated at pH < 1.2, it was an amorphous hydrated phase, UO_2(am, hyd), at pH ≥ 1.2. (Manfredi et al., 2006) determined the hydrolysis constants of U(IV) by potentiometry in the absence of a solid phase. A controlled setup with specific ionic strength and pH conditions was used. The obtained hydrolysis constants in the reference state reported for the (1,1) and (1,4) hydrolysis species ($\log_{10}{}^*\beta_1^\circ$ and $\log_{10}{}^*\beta_4^\circ$) are consistent with those selected in the NEA-TDB. (Opel et al., 2007) conducted a careful study by coulometric titration to determine the solubility of U(IV) in $HClO_4$/$NaClO_4$ solutions. The solubility products were found to be dependent on the particle size of colloids determined by laser-induced breakdown detection (LIBD). (Fellhauer et al., 2010) investigated the solubility and hydrolysis of Np(IV) and Pu(IV) in dilute to concentrated $CaCl_2$ solutions. Analogously to the ternary aqueous complexes Ca-An(IV)–OH previously reported for Th(IV), the authors reported the equilibrium constants and SIT/Pitzer ion interaction coefficients for the complexes $Ca_4[An(OH)_8]^{4+}$ (with An = U, Np, and Pu) based on experimental solubility data and linear free energy relationships. (Cevirim-Papaioannou, 2018) conducted a comprehensive study on the solubility and hydrolysis of U(IV) in reducing, dilute to concentrated NaCl, $MgCl_2$, and $CaCl_2$ solutions. The author used a solid phase aged under reducing conditions and conducted long-term solubility experiments with up to 351 days of equilibration time. U solid phases were comprehensively characterized using a multi-method approach, including powder X-ray diffraction analysis (XRD), scanning electron microscopy (SEM) and energy dispersive X-ray spectroscopy (EDS), thermogravimetry differential thermal analysis (TG/DTA), and X-ray absorption near edge structure (XANES)/extended X-ray absorption fine structure (EXAFS). Besides the experimental studies described above, it is important to note that the U(IV) hydrolysis constants selected in the main thermodynamic databases in the context of nuclear waste disposal, e.g., THEREDA (Moog et al., 2015), ThermoChimie (Giffaut et al., 2014), PSI/Nagra Chemical Thermodynamic Database (Hummel and Thoenen, 2023) or Japan Atomic Energy Agency - Thermodynamic Database (JAEA-TDB) (Kitamura, 2021), strongly rely on the thermodynamic data selection provided in the NEA-TDB reviews (Grenthe et al., 1992, 2020; Guillaumont et al., 2003). The formation of U(IV) chloro-complexes has been confirmed by spectroscopic means, and thermodynamic data for the complex UCl^{3+} has been selected in the NEA-TDB as well as in all SIT-based thermodynamic databases. In contrast to this, previous studies using the Pitzer formalism to describe An(IV) solubility and hydrolysis in dilute to concentrated chloride systems disregard An(IV) chloro-complexes in the chemical model, exclusively describing this interaction through the activity model (Neck et al., 2001; Rai et al., 1997). This is also the approach considered in the Pitzer-based thermodynamic database THEREDA (Moog et al., 2015).

Despite the wealth of existing experimental and theoretical studies, significant gaps remain in our understanding of U(IV) behavior, particularly in chloride-rich environments. The ageing of U(IV) hydrous oxide phases, as well as ion-ion interaction processes at high chloride concentrations and their impact on U(IV) solubility and hydrolysis need to be accurately modeled. Building upon the foundation laid by the previous studies, this work undertakes the task of updating the available thermodynamic and Pitzer activity models for the description of U(IV) solubility and hydrolysis in dilute to concentrated chloride systems. Using the NEA-TDB selection as anchoring point, this modelling work is based on the comprehensive solubility studies conducted by (Cevirim-Papaioannou, 2018; Rai et al., 1997) in dilute to concentrated NaCl, $MgCl_2$, and $CaCl_2$ systems. All equilibrium constants and model calculations described in this work correspond to $T = 25$ °C.

2. Pitzer formalism for the description of high saline systems

The Pitzer formalism allows the precise determination of activity coefficients of individual ions within complex mixed electrolyte systems extending to high ionic strength conditions. Readers are referred to the primary works by Pitzer (Pitzer, 1973, 1975, 1991; Pitzer and Kim, 1974; Pitzer and Mayorga, 1973, Pitzer and Mayorga, 1974) and relevant review literature for an in-depth understanding of Pitzer equations and the underlying physical principles.

Pitzer equations include binary parameters describing specific anion-cation interactions, i.e., $\beta_{MX}^{(0)}$, $\beta_{MX}^{(1)}$, $\beta_{MX}^{(2)}$ and $C_{MX}^{(\varphi)}$. $\beta_{MX}^{(0)}$ and $\beta_{MX}^{(1)}$ refer to short-range interactions, whereas $\beta_{MX}^{(2)}$ is $\neq 0$ exclusively for 2–2 electrolyte systems, showcasing a remarkable correlation with the ion association constants that characterize these specific ion pairs. The parameters θ_{Mc} and θ_{Xa} describe asymmetric mixing with interactions between unlike cation-cation and anion-anion pairs, respectively. Ψ_{cXa} and Ψ_{Mca} are third virial coefficients representing triple interactions between ions c, X, a (two different anions and a cation) or M, c, a (two different cations and an anion). The interplay between ions and neutral species is accounted for by the parameters λ_{nM} and λ_{nX}.

Due to the multitude of binary and ternary parameters required to calculate activity coefficients using the Pitzer equations, activity models derived on the basis of this formalism necessitate extensive experimental datasets covering substantial variations in background electrolyte concentrations. These prerequisites notably influence the formulation of Pitzer activity models in radionuclide systems, where existing datasets often encompass only a handful of background electrolyte concentrations. To address these constraints and, notably, to prevent over-parameterization of these limited datasets, certain simplification approaches and estimation methods have been devised and documented in prior studies (Grenthe et al., 1997; Plyasunov et al., 1998; Yalçıntaş et al., 2019).

THEREDA is designed for geochemical model calculations in the context of radioactive waste disposal (Moog et al., 2015). THEREDA especially addresses high-salinity/brine systems, and it is accordingly built on the basis of Pitzer activity models. The primary focus is on the correct calculation of the solubilities of radionuclides, fission products, and matrix elements. The present study is part of the systematic development of the THEREDA database. In line with the previous U(IV) Pitzer model in THEREDA, this work has considered only the binary Pitzer parameters for the U(IV) aqueous complexes, i.e., $\beta_{MX}^{(0)}$, $\beta_{MX}^{(1)}$ and $C_{MX}^{(\varphi)}$. All binary and ternary Pitzer parameters required for the $HCl–NaCl–MgCl_2–CaCl_2–NaOH–Mg(OH)_2\text{-}Ca(OH)_2\text{-}H_2O(l)$ systems have been taken from the THEREDA database (Moog et al., 2015), and are summarized in Tables S1 and S2 in the Supporting Information.

3. Methods

3.1. Experimental data considered in this work

Solubility data reported in the literature for hydrous $UO_2(s)$ are very scattered, reflecting the different character of the solid phases controlling the solubility in the different studies, in particular differences in particle size. Most of the studies focus on dilute systems and only two of them, *i.e.* (Rai et al., 1997; Cevirim-Papaioannou, 2018), covered concentrated chloride solutions beyond 1 mol/L NaCl. Due to the extensive solid phase characterization conducted in (Cevirim-Papaioannou, 2018), the comprehensive dataset in 0.1, 0.5, 2.0, 5.0 mol/L NaCl and 0.25, 2.0 and 4.5 mol/L $MgCl_2$/$CaCl_2$ has been considered in this work for the update of the thermodynamic and Pitzer activity models currently selected in THEREDA. The systematic solubility study by (Rai et al., 1997) in NaCl and $MgCl_2$ solutions is compared with model predictions using thermodynamic and Pitzer activity models derived in this work.

A noteworthy observation in the solubility data reported by (Cevirim-Papaioannou, 2018) is the presence of aged solid phases exhibiting significantly lower solubility compared to the UO_2(am, hyd) solid phase selected in the NEA-TDB or reported in the shorter experiments conducted (Rai et al., 1997). On the basis of a multi-method approach (XRD, TG-DTA, XAFS) used for the characterization of the solid phase after completing the solubility experiments, the aged solid phase in (Cevirim-Papaioannou, 2018) was identified as nanocrystalline $UO_2{\bullet}H_2O$(ncr).

3.2. Strategy for the development of the thermodynamic and pitzer activity models

The aqueous speciation of U(IV) in the absence of complexing ligands is defined by a chemical model that includes the aqueous species U^{4+}, UOH^{3+}, $U(OH)_2^{2+}$, $U(OH)_3^+$, and $U(OH)_4$(aq), along with the solid phases $UO_2{\bullet}2H_2O$(am,hyd) (quoted as UO_2(am, hyd) in the NEA-TDB) or $UO_2{\bullet}H_2O$(ncr). Consistently with previous Pitzer studies and with the strategy adopted in THEREDA for all An(IV), the interaction of U(IV) with chloride is exclusively described through binary Pitzer coefficients [16, 25–26]. This approach aims at avoiding the overparameterization in the fit of the available datasets. The ternary complex $Ca_4[An(OH)_8]^{4+}$ previously described for Th(IV) (Altmaier et al., 2008), Np(IV), and Pu (IV) (Fellhauer et al., 2010) has been included to account for the speciation of U(IV) in dilute to concentrated $CaCl_2$ solutions. Given the large number of parameters required to describe the solubility and hydrolysis of U(IV) (log ${}^{*}K^0_{s,0}$, ${}^{*}\beta^0_{(1,1)}$, ${}^{*}\beta^0_{(1,2)}$, ${}^{*}\beta^0_{(1,3)}$, ${}^{*}\beta^0_{(1,4)}$ and the corresponding Pitzer coefficients for U^{4+}, UOH^{3+}, $U(OH)_2^{2+}$, $U(OH)_3^+$, and U $(OH)_4$(aq)), the following modeling approach is considered in the present work:

- Equilibrium constants are taken as reported in the NEA-TDB $({}^{*}K^0_{s,0}(UO_2 \bullet 2H_2O(am))$; ${}^{*}\beta^0_{(1,1)}$; ${}^{*}\beta^0_{(1,2)}$; ${}^{*}\beta^0_{(1,3)}$; ${}^{*}\beta^0_{(1,4)}$), (Cevirim-Papaioannou, 2018; ${}^{*}K^0_{s,0}\left(UO_2 \bullet H_2O(ncr)\right)$ Fellhauer et al., 2010 ${}^{*}K^0_{s,0}\left(UO_2 \bullet H_2O(ncr)\right)$ $\left({}^{*}\beta^0_{(4,1,8)}\right)$.
- The U(IV) Pitzer model currently selected in THEREDA is taken as basis for the optimization process. The species U^{4+}, UOH^{3+}, and U $(OH)_3^+$ are expected to play a relatively minor role in the pH-range considered in (Cevirim-Papaioannou, 2018; Rai et al., 1997), as can be seen in the Supporting Information (Fig. S1). For this reason, only an optimization of the Pitzer parameters β_0, β_1, and C^{Φ} of the species $U(OH)_2^{2+}$ has been considered.
- Matlab (MATLAB, 2022) was used for the fitting process through a multi-fitting algorithm, i.e., the NLINMULTIFIT function, which operates a non-linear least squares regression of multiple data sets (Chen, 2016). All of the datasets reported by (Cevirim-Papaioannou, 2018) are simultaneously fitted using the minimization function $\sum \left(\log [U]_{exp} - \log [U]_{calc}\right)^2 \left(\log [U]_{exp} - \log [U]_{calc}\right)^2$. The NLINFIT Matlab function operates the simultaneous fitting of multiple non-linear curves with shared parameters. Fig. S2 in the Supporting Information provides a flow diagram described the approach used for the fit of the available experimental data. The outcome of this fitting exercise was counterchecked using The Geochemist's Workbench code (Bethke, 2023). The value of $[U]_{calc}$ is the sum of $[U^{4+}]$, $[UOH^{3+}]$, $[U(OH)_2^{2+}]$, $[U(OH)_3^+]$, and $[U(OH)_4(aq)]$, as exemplarily described for $UO_2{\bullet}H_2O$(ncr) in equations (17)–(24):

$$UO_2 \bullet H_2O(ncr) + 4H^+ \rightleftharpoons U^{4+} + 3H_2O(l) \tag{17}$$

$$UO_2 \bullet H_2O(ncr) + 3H^+ \rightleftharpoons U(OH)^{3+} + 2H_2O(l) \tag{18}$$

$$UO_2 \bullet H_2O(ncr) + 2H^+ \rightleftharpoons U(OH)_2^{2+} + H_2O(l) \tag{19}$$

$$UO_2 \bullet H_2O(ncr) + H^+ \rightleftharpoons U(OH)_3^+ \tag{20}$$

$$UO_2 \bullet H_2O(ncr) + H_2O(l) \rightleftharpoons U(OH)_4(aq) \tag{21}$$

$${}^{*}K^0_{s,0} = a_{U^{4+}} \bullet {a_w}^3 \bullet {a_{H^+}}^{-4} \tag{22}$$

$${}^{*}\beta^0_{(1,n)} = a_{U(OH)_n^{4-n}} \bullet {a_{H^+}}^{n} \bullet {a_w}^{-n} \bullet {a_{U^{4+}}}^{-1} \tag{23}$$

$$[U]_{calc} = {}^{*}K^0_{s,0} \bullet {\gamma_{H^+}}^4 \bullet {m_{H^+}}^4 \bullet {a_w}^{-3} \bullet {\gamma_{U^{4+}}}^{-1} \left(1 + \sum {}^{*}\beta^0_{(1,n)} \bullet \gamma_{U^{4+}} \bullet {m_{H^+}}^{-n} \bullet {\gamma_{H^+}}^{-n} \bullet {\gamma_{U(OH)_n^{4-n}}}^{-1} \bullet {a_w}^{n}\right) \tag{24}$$

Note that the provision of thermodynamic data for amorphous solid phases entails some challenging aspects, as their solubility may change with time due to re-crystallisation and consequent decrease in water content and surface area. However, having access to the solubility of amorphous phases is of utmost importance when modelling the behaviour of complex systems. For this reason and following the philosophy of the NEA-TDB reference books (Guillaumont et al., 2003), solubility products of U(IV) amorphous and hydrated oxyhydroxide phases are provided in this work.

4. Results and discussion

4.1. Modeling of $UO_2(s)$ solubility in dilute to concentrated NaCl systems

Fig. 1 shows the experimental solubility data reported by (Cevirim-Papaioannou, 2018; Rai et al., 1997) for dilute to concentrated NaCl solutions, together with the solubility calculations using the thermodynamic and Pitzer activity models derived in this work.

Uranium concentrations determined by (Cevirim-Papaioannou, 2018) are about 2 orders of magnitude lower than those reported in (Rai et al., 1997), reflecting the larger particle size of the solid phase reported in (Cevirim-Papaioannou, 2018). It is worth noting that the solid phase used by (Cevirim-Papaioannou, 2018) underwent aging for 3 months before initiating the undersaturation solubility experiments, which were conducted for a significantly longer timeframe compared to previous solubility studies (Neck and Kim, 2001; Rai et al., 1997). This highlights the necessity of defining two different solid phase stabilities in the thermodynamic data selection, *i.e.* one for $UO_2{\bullet}2H_2O$(am) (equivalent to UO_2(am, hyd) selected in the NEA-TDB) and one for $UO_2{\bullet}H_2O$(ncr). The ageing effects observed for fresh amorphous precipitates may be interpreted in terms of increasing particle size by surface recrystallization via local dissolution-precipitation equilibria (Ostwald ripening) (Rand et al., 2008). Although the NEA-TDB currently selects solubility constants for only one U(IV) hydrous oxide (UO_2(am, hyd)) (Grenthe

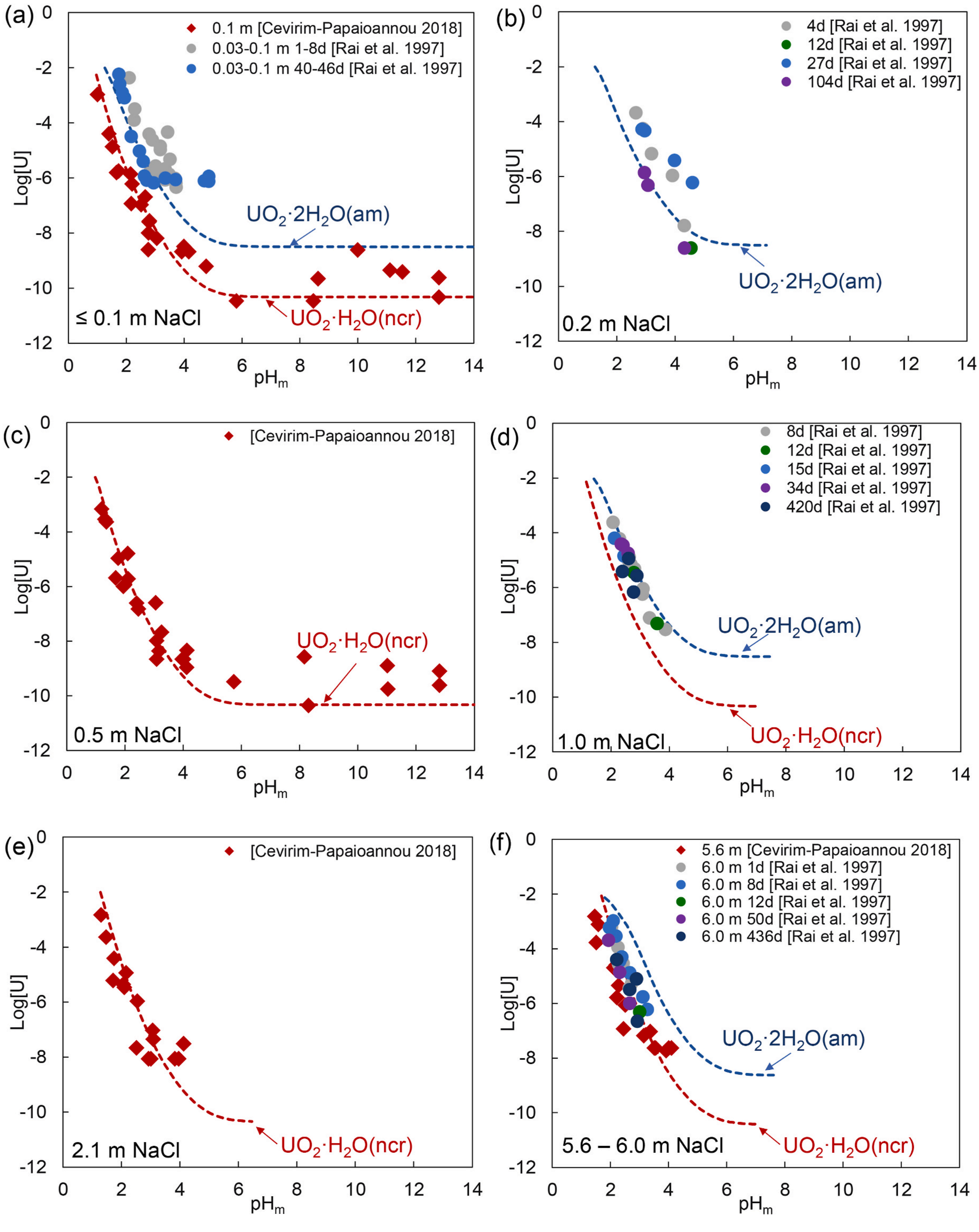

Fig. 1. Comparison of model calculations with experimental U(IV) solubility data reported in (Cevirim-Papaioannou, 2018; Rai et al., 1997) for (a) ≤ 0.1, (b) 0.2, (c) 0.5, (d) 1.0, (e) 2.1 and (f) 5.6–6.0 mol/kg NaCl solutions. Solubility calculations represented by dashed lines are conducted with thermodynamic and Pitzer activity models selected in the present work.

et al., 2020), the two solid phases defined in this work for U(IV) can be considered analogous to those currently selected for Th(IV) in the NEA-TDB and THEREDA databases, *i.e.* ThO_2(am, hyd, fresh) and ThO_2(am, hyd, aged) (Moog et al., 2015; Rand et al., 2008).

The solubility of U(IV) in the acidic pH region increases with increasing NaCl concentrations, reflecting strong ionic interactions of the positively charged U(IV) hydrolysis species with chloride, as shown in Fig. S3 in the Supporting Information. Experimental solubility data reported by (Cevirim-Papaioannou, 2018) and solubility calculations performed with the thermodynamic and Pitzer activity models derived in this work are in excellent agreement for the complete range of ionic strength conditions, *i.e.* 0.1–5.6 mol/kg, considering $UO_2{\bullet}H_2O$(ncr) as solid phase controlling the solubility. Model calculations considering $UO_2{\bullet}2H_2O$(am) and experimental data reported by (Rai et al., 1997) are also in good agreement for dilute to intermediate ionic strength conditions, *i.e.* 0.03 mol/kg to 1.0 mol/kg. For the highest NaCl concentration investigated (Rai et al., 1997) (6.0 mol/kg NaCl), solubility data agree with that reported in (Cevirim-Papaioannou, 2018) and with solubility calculations considering $UO_2\bullet H_2O$(ncr) as solid phase controlling the solubility of U(IV). We speculate that an increase in particle size may have occurred during the solubility experiments at high chloride concentrations.

4.2. Modeling of UO_2(s) solubility in dilute to concentrated $MgCl_2$ systems

Fig. 2 illustrates the solubility calculations using the thermodynamic and Pitzer activity models derived in this work, along with the experimental solubility data reported by (Cevirim-Papaioannou, 2018; Rai et al., 1997) for dilute to concentrated $MgCl_2$ solutions. Under acidic

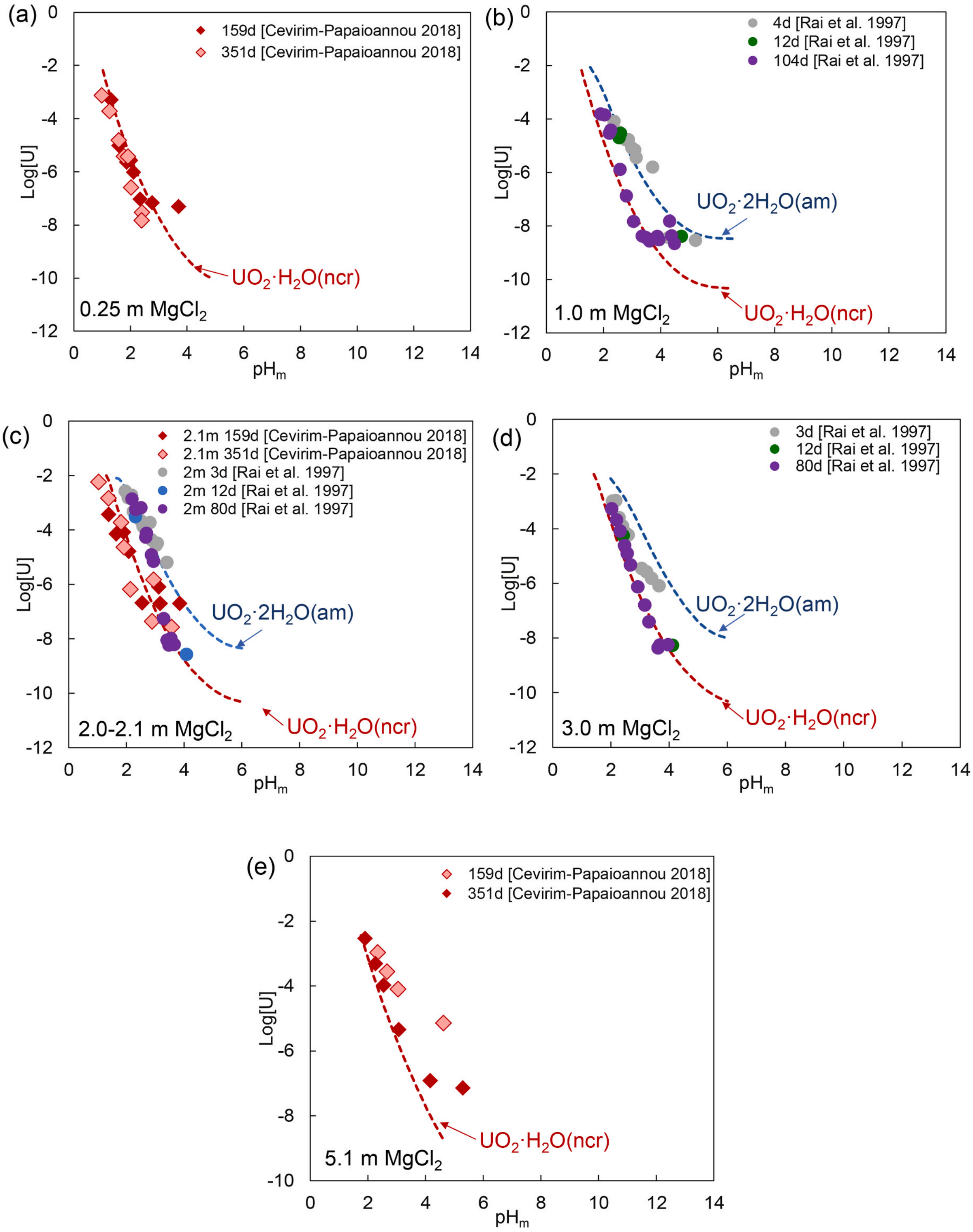

Fig. 2. Comparison of model calculations with experimental U(IV) solubility data reported in (Cevirim-Papaioannou, 2018; Rai et al., 1997) for (a) 0.25, (b) 1.0, (c) 2.0–2.1, (d) 3.0 and (e) 5.1 mol/kg $MgCl_2$ solutions. Solubility calculations represented by dashed lines are conducted with thermodynamic and Pitzer activity models selected in the present work.

conditions ($pH_m \leq 4$) and analogous to the NaCl systems, a steep decrease in the solubility of U(IV) is observed with increasing pH_m in all $MgCl_2$ systems. The increase in $MgCl_2$ concentration results in a significant increase in the solubility (ca. 3 orders of magnitude from 0.25 to 5.15 mol/kg $MgCl_2$), as shown in Fig. S4 in the Supporting Information. Such a relevant increase in the solubility expectedly results from strong ion interaction processes.

Similar to NaCl systems, uranium concentrations in acidic $MgCl_2$ solutions determined by (Cevirim-Papaioannou, 2018) are approximately 2 orders of magnitude lower than those reported by (Rai et al., 1997), confirming again the larger particle size, i.e. greater stability, of the solid phase used by (Cevirim-Papaioannou, 2018). As in the NaCl systems, solubility calculations using thermodynamic and Pitzer activity models derived in this work show a very good agreement with the experimental solubility data reported (Cevirim-Papaioannou, 2018) for the complete range of ionic strength conditions, *i.e.* 0.75–13.5 mol/kg, considering $UO_2{\bullet}H_2O$(ncr) as solid phase controlling the U(IV) solubility. This observation supports the idea that the same kind of nanocrystalline solid phase is responsible for the control of U(IV) solubility in both salt systems. For some of the experimental data reported (Rai et al., 1997) (1.0 mol/kg $MgCl_2$ 104 d; 2.0 mol/kg $MgCl_2$ 12 d and 80 d; and 3.0 mol/kg $MgCl_2$), long-term solubility data agree with that reported (Cevirim-Papaioannou, 2018) and with solubility calculations considering $UO_2{\bullet}H_2O$(ncr) as solid phase controlling the solubility of U(IV). This observation reinforces the hypothesis of an increase in particle size in the course of the solubility experiments (Rai et al., 1997), which is especially relevant at higher chloride concentrations. We hypothesize that this effect may be caused by the enhanced solubility triggered by ionic interaction effects in concentrated chloride media, which can accelerate particle growth through faster recrystallization kinetics.

At $pH_m \geq 3$–4 (depending on $MgCl_2$ concentration and solid phase controlling the solubility), the uranium concentration in equilibrium with $UO_2{\bullet}H_2O$(ncr) or $UO_2{\bullet}2H_2O$(am) drops below the detection limit of Inductively coupled plasma mass spectrometry (ICP-MS), and thus no information could be gained for this salt system and pH_m range (Cevirim-Papaioannou, 2018). Nevertheless, based on the results obtained in NaCl systems and data reported for the solubility of Th(IV) in $MgCl_2$ systems (Altmaier et al., 2004), a solubility control by the pH_m-independent solubility reaction $UO_2(s, hyd) \rightleftharpoons U(OH)_4(aq) + xH_2O(l)$ is expected.

4.3. Modeling of $UO_2(s)$ solubility in dilute to concentrated $CaCl_2$ systems

The contact of concentrated $MgCl_2$ solutions with cement at a given solid/brine ratio can result in the formation of concentrated $CaCl_2$ solutions (2–3.5 mol/kg) with pH_m values close to 12 (Bube et al., 2013) (see Fig. 3). At solid/brine ratios >1 g/mL, (Bube et al., 2013) confirmed that the main phases remaining after exposure to $MgCl_2$ were brucite, Friedel's salt, Ca-oxychloride, $Ca_4Si_3O_{10}{\bullet}1.5H_2O$, gypsum, and calcite.

(Cevirim-Papaioannou, 2018) investigated also the solubility of U(IV) in alkaline, dilute to concentrated $CaCl_2$ solutions, but all measured uranium concentrations were at the detection limit of ICP-MS for the given salt concentrations (see Fig. 4). (Fellhauer et al., 2010) reported a thermodynamic model for U(IV) based on Linear Free-Energy Relationships (LFER) and experimental solubility data determined in $CaCl_2$ systems for Th(IV), Np(IV), and Pu(IV). This model has been considered in the current data selection, and is used for the solubility calculations in Fig. 4, considering $UO_2{\bullet}H_2O$(ncr) as solid phase controlling the solubility. Experimental solubility data (basically all data points at the detection limit of the technique) are not in disagreement with the calculated solubility. These experimental observations are justified by the low solubility of $UO_2{\bullet}H_2O$(ncr) and the strong dilutions required for ICP-MS measurements in concentrated $CaCl_2$. As for Th(IV), Np(IV), and Pu(IV), thermodynamic calculations predict the predominance of the ternary complex $Ca_4[An(OH)_8]^{4+}$ in hyperalkaline solutions with a salt concentration ≥2.1 mol/kg $CaCl_2$ (see Fig. 4).

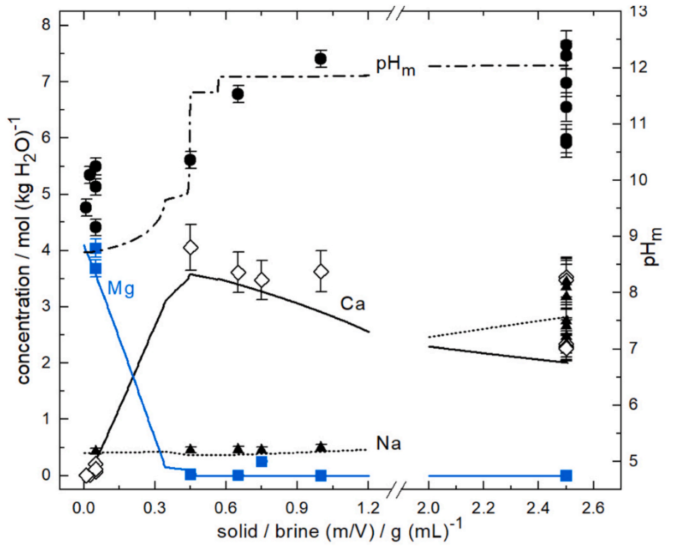

Fig. 3. Evolution of the pore water of a cement drum exposed to increasing volumes of $MgCl_2$ brine as reported by (Bube et al., 2013). Solid lines refer to thermodynamic calculations considering the predominance of the solid phases reported in the text. Figure modified from (Bube et al., 2013).

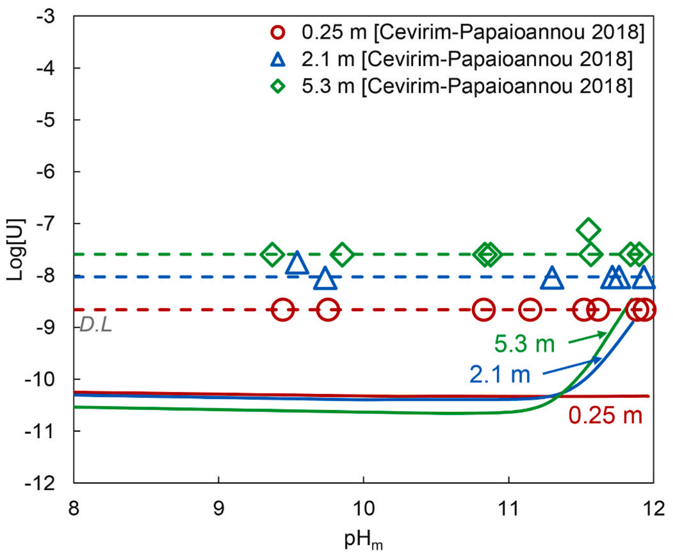

Fig. 4. Comparison of model calculations with experimental U(IV) solubility data reported in (Cevirim-Papaioannou, 2018) for 0.25, 2.1, and 5.3 mol/kg $CaCl_2$ solutions. Solubility calculations represented by solid lines are conducted with thermodynamic and Pitzer activity models selected in the present work. Dashed lines are detection limits (D.L.) of ICP–MS as described in (Cevirim-Papaioannou, 2018).

4.4. Thermodynamic and pitzer activity models for the system U^{4+}–Na^+–Mg^{2+}–Ca^{2+}–H^+–Cl^-–OH^-–$H_2O(l)$: Incorporation in the THEREDA-TDB

Table 1 summarizes the solubility and hydrolysis constants of U(IV) as selected in the previous THEREDA-TDB and in this study. The new thermodynamic model considers the NEA-TDB thermodynamic selection as anchoring point, whilst defining two solid phases, i.e., $UO_2{\cdot}2H_2O$(am) and $UO_2{\cdot}H_2O$(ncr, hyd). This allows to the proper description of most of the experimental solubility data available in dilute to concentrated NaCl, $MgCl_2$, and $CaCl_2$ solutions.

Table 2 summarizes the Pitzer coefficients for U(IV) hydrolysis species as previously selected in THEREDA-TDB and reported in this study.

Table 1
Equilibrium constants of U(IV) solubility and hydrolysis selected in the previous THEREDA-TDB and this study.

		Previous THEREDA-TDB	Original source	This study	Original source
Solubility	$UO_2{\cdot}2H_2O(am, hyd) + 4H^+ \rightleftharpoons U^{4+} + 4H_2O(l)$	(1.5 ± 1.0)	NEA-TDB (Guillaumont et al., 2003)	(1.5 ± 1.0)	NEA-TDB (Grenthe et al., 2020)
	$UO_2{\cdot}H_2O(ncr) + 4H^+ \rightleftharpoons U^{4+} + 3H_2O(l)$	–	–	–(0.32 ± 0.60)	Cevirim-Papaioannou (Cevirim-Papaioannou, 2018)
Hydrolysis constants, $\log_{10}{}^*\beta_n^0$	$U^{4+} + H_2O(l) \rightleftharpoons U(OH)^{3+} + H^+$	–(0.54 ± 0.06)	NEA-TDB (Guillaumont et al., 2003)	–(0.54 ± 0.06)	NEA-TDB (Grenthe et al., 2020)
	$U^{4+} + 2H_2O(l) \rightleftharpoons U(OH)_2^{2+} + 2H^+$	–(1.1 ± 1.0)	Neck and Kim (Neck and Kim, 2001), estimated	–(1.9 ± 0.2)	NEA-TDB (Grenthe et al., 2020)
	$U^{4+} + 3H_2O(l) \rightleftharpoons U(OH)_3^+ + 3H^+$	–(4.7 ± 1.0)	Neck and Kim (Neck and Kim, 2001), estimated	–(5.2 ± 0.4)	NEA-TDB (Grenthe et al., 2020)
	$U^{4+} + 4H_2O(l) \rightleftharpoons U(OH)_4(aq) + 4H^+$	–(10 ± 1.4)	NEA-TDB (Guillaumont et al., 2003)	–(10 ± 1.4)	NEA-TDB (Grenthe et al., 2020)
	$4Ca^{2+} + U^{4+} + 8H_2O(l) \rightleftharpoons Ca_4[U(OH)_8]^{4+} + 8H^+$	–	–	–(59.5 ± 1.0)	Fellhauer (Fellhauer et al., 2010), estimated

Table 2
Pitzer interaction coefficients in the previous THEREDA-TDB and this study.

	Ion 1	Ion 2	β_0	β_1	C^Φ	Primary reference
Previous THEREDA-TDB	U^{4+}	Cl^-	1.27	13.5		Neck et al. (2001)
	$U(OH)^{3+}$	Cl^-	0.6	5.9		Neck et al. (2001)
	$U(OH)_2^{2+}$	Cl^-	0.23	1.93		Neck et al. (2001)
	$U(OH)_3^+$	Cl^-	0.08	0.39		Neck et al. (2001)
This work	U^{4+}	Cl^-	1.27	13.5	0	Neck et al. (2001)
	$U(OH)^{3+}$	Cl^-	0.6	5.9	0	Neck et al. (2001)
	$U(OH)_2^{2+}$	Cl^-	0.37	1.93	−0.029	Fit of exp. Data, this work
	$U(OH)_3^+$	Cl^-	0.08	0.39	0	Neck et al. (2001)
	$Ca_4[U(OH)_8]^{4+}$	Cl-	0.58	8.9	0.07	(Fellhauer et al., 2010), analogy with other An (IV)

Only parameters available for $U(OH)_2^{2+}$ have been modified on the basis of the new experimental solubility data, whereas binary parameters for $Ca_4[U(OH)_8]^{4+}$ are taken from the LFER estimates reported by Fellhauer and co-workers (Fellhauer et al., 2010).

5. Summary and conclusions

This study presents updated chemical, thermodynamic, and Pitzer activity models for the system U^{4+}–Na^+–Mg^{2+}–Ca^{2+}–H^+–Cl^-–OH^-–H_2O(l). These models disregard association equilibria involving chloride, and are based on the most comprehensive experimental dataset available to date for U(IV) in dilute to concentrated NaCl, $MgCl_2$, and $CaCl_2$ solutions. Two U(IV) hydrous oxides ($UO_2{\cdot}2H_2O$(am) and $UO_2{\cdot}H_2O$(ncr)) with different stability are considered in the model, reflecting the increase in particle size and consequent decrease in solubility that a freshly precipitated solid phase undergoes through the Ostwald ripening triggered by ageing. This is in line with the selection of thermodynamic data for ThO_2(am, hyd, fresh) and ThO_2(am, hyd, aged) as considered in most databases available for nuclear waste disposal applications (NEA-TDB, ThermoChimie, PSI-Nagra, JAEA, THEREDA, etc.). The current NEA-TDB selection for the solubility and hydrolysis constants in the reference state, i.e. ${}^*K^0_{s,0}(UO_2 \bullet 2H_2O(am))$, ${}^*\beta^0_{(1,1)}$, ${}^*\beta^0_{(1,2)}$, ${}^*\beta^0_{(1,3)}$, ${}^*\beta^0_{(1,4)}$, is considered as anchoring point in the development of the thermodynamic model. The ternary complex $Ca_4[An(OH)_8]^{4+}$ has been included in the thermodynamic selection based on experimental evidences available in the literature for Th(IV), Np(IV), and Pu(IV). This complex may become predominant in cementitious systems contacted with $MgCl_2$ brines, in which high $CaCl_2$ concentrations can be attained. The Pitzer model derived in this work builds on the previous selection in THEREDA, and includes the optimizations of the Pitzer parameters β_0, β_1, and C^Φ of $U(OH)_2^{2+}$.

The chemical, thermodynamic, and activity models derived in this work enable robust and precise solubility calculations, serving as a valuable tool for source term estimations in the geochemical assessment of repositories for nuclear waste disposal. Notably, this work provides a reliable Pitzer activity model that can be confidently applied up to concentrated brines and pH_m conditions potentially expected in disposal concepts in salt rock or specific clay formations present in Canada or Northern Germany.

CRediT authorship contribution statement

Y. Yan: Writing – review & editing, Writing – original draft, Methodology, Investigation, Formal analysis. **N. Cevirim-Papaioannou:** Writing – review & editing, Methodology, Investigation, Data curation. **X. Gaona:** Writing – review & editing, Supervision, Project administration, Methodology, Funding acquisition, Conceptualization. **D. Fellhauer:** Writing – review & editing, Supervision, Formal analysis, Conceptualization. **M. Altmaier:** Writing – review & editing, Project administration, Funding acquisition, Conceptualization.

Declaration of competing interest

The authors declare the following financial interests/personal relationships which may be considered as potential competing interests:

KIT-INE reports financial support was provided by Bundesgesellschaft für Endlagerung (BGE). If there are other authors, they declare that they have no known competing financial interests or personal relationships that could have appeared to influence the work reported in this paper.

Data availability

Data will be made available on request.

Acknowledgements

This work was funded by the Bundesgesellschaft für Endlagerung (BGE) as part of the activities related to THEREDA (www.thereda.de).

Appendix A. Supplementary data

Supplementary data to this article can be found online at https://doi.org/10.1016/j.apgeochem.2024.106091.

References

Altmaier, M., Gaona, X., Fanghänel, T., 2013. Recent advances in aqueous actinide chemistry and thermodynamics. Chem. Rev. 113, 901–943.

Altmaier, M., Neck, V., Fanghänel, T., 2008. Solubility of Zr(IV), Th(IV) and Pu(IV) hydrous oxides in CaCl2 solutions and the formation of ternary Ca-M(IV)-OH complexes. Radiochim. Acta 96, 541–550.

Altmaier, M., Neck, V., Fanghänel, T., 2004. Solubility and colloid formation of Th(IV) in concentrated NaCl and MgCl2 solution. Radiochim. Acta 92, 537–543.

Bethke, C.M., 2023. The Geochemist's Workbench®. https://www.gwb.com/downloads.php.

Brewitz, W., 1980. GSF-T 114; Ges. F. Strahlen-U.

Bruno, J., Casas, I., Lagerman, B., Munoz, M., 1986. The determination of the solubility of amorphous UO2 (s) and the mononuclear hydrolysis constants of uranium(IV) at 25° C. MRS Online Proc. Libr. 84, 153–160.

Bube, C., Metz, V., Bohnert, E., Garbev, K., Schild, D., Kienzler, B., 2013. Long-term cement corrosion in chloride-rich solutions relevant to radioactive waste disposal in rock salt - Leaching experiments and thermodynamic simulations. Phys. Chem. Earth 64, 87–94.

Cevirim-Papaioannou, N., 2018. Redox Chemistry, Solubility and Hydrolysis of Uranium in Dilute to Concentrated Salt Systems. Ph.D. Thesis. KIT, Karlsruhe. https://publikationen.bibliothek.kit.edu/1000084978.

Çevirim-Papaioannou, N., Yalçıntaş, E., Gaona, X., Dardenne, K., Altmaier, M., Geckeis, H., 2018. Redox chemistry of uranium in reducing, dilute to concentrated NaCl solutions. Appl. Geochem. 98, 286–300.

Chen, Avinadav, 2016. Multiple Curve Fitting with Common Parameters Using NLINFIT. https://www.mathworks.com/matlabcentral/fileexchange/40613-multiple-curve-fitting-with-common-parameters-using-nlinfit.

Ciavatta, L., 1980. The specific interaction theory in evaluating ionic equilibria. Ann. Chim. 70, 551.

Fellhauer, D., Neck, V., Altmaier, M., Lützenkirchen, J., Fanghänel, T., 2010. Solubility of tetravalent actinides in alkaline CaCl2 solutions and formation of Ca4[An(OH)8]4+ complexes: a study of Np(IV) and Pu(IV) under reducing conditions and the systematic trend in the An(IV) series. Radiochim. Acta 98, 541–548.

Frape, S.K., Fritz, P., McNutt, R.H., 1984. Water-rock interaction and chemistry of groundwaters from the Canadian Shield. Geochem. Cosmochim. Acta 48, 1617–1627.

Fujiwara, K., Yamana, H., Fujii, T., Kawamoto, K., Sasaki, T., Moriyama, H., 2007. Solubility of uranium(IV) hydrous oxide in high pH solution under reducing condition. Radiochim. Acta 93, 347–350.

Fujiwara, K., Yamana, H., Fujii, T., Moriyama, H., 2003. Determination of uranium(IV) hydrolysis constants and solubility product of UO2·xH2O. Radiochim. Acta 91, 345–350.

Galkin, N.P., Stepanov, M.A., 1961. Solubility of uranium (IV) hydroxide in sodium hydroxide. Sov. J. At. Energy 8, 231–233.

Gayer, K.H., Leider, H., 1957. The solubility of thorium hydroxide in solutions of sodium hydroxide and perchloric acid at 25. J. Am. Chem. Soc. 76, 5938–5940. https://pubs.acs.org/doi/pdf/10.1021/ja01652a012.

Giffaut, E., Grivé, M., Blanc, P., Vieillard, P., Colàs, E., Gailhanou, H., Gaboreau, S., Marty, N., Madé, B., Duro, L., 2014. Andra thermodynamic database for performance assessment: ThermoChimie. Appl. Geochem. 49, 225–236.

Grenthe, I., Fuger, J., Konings, R.J.M., Lemire, R.J., Muller, A.B., Gregu, C.N.-T., Wanner, H., 1992. Chemical Thermodynamics of Uranium. OECD Nuclear Energy Agency.

Grenthe, I., Gaona, X., Plyasunov, A.V., Rao, L., Runde, W.H., Grambow, B., Konings, R.J.M., Smith, A.L., Moore, E.E., 2020. Second Update on the Chemical Thermodynamics of Uranium, Neptunium, Plutonium, Americium and Technetium. https://www.oecd-ilibrary.org/nuclear-energy/second-update-on-the-chemical-thermodynamics-of-uranium-neptunium-plutonium-americium-and-technetium-volume-14_bf86a907-en.

Grenthe, I., Puigdomenech, I., Allard, B., 1997. OECD nuclear energy Agency. Modelling in Aquatic Chemistry. Nuclear Energy Agency, Organisation for Economic Co-operation and Development. https://www.oecd-nea.org/dbtdb/pubs/modelling-aquatic-chem.html.

Guillaumont, R., Fanghänel, T., Neck, V., Fuger, J., Palmer, D.A., Grenthe, I., Rand, M., 2003. Update on the Chemical Thermodynamics of Uranium, Neptunium, Plutonium, Americium and Technetium. OECD Nuclear Energy Agency. https://www.semanticscholar.org/paper/Update-on-the-chemical-thermodynamics-of-uranium%2C-Guillaumont-Mompe%C3%A1n/26146b21c3b18bb96dc19cfb64bffc613ddc883a.

Hummel, W., Thoenen, T., 2023. Nagra Technical Report 21-03: the PSI Chemical Thermodynamic Database 2020. Wettingen. https://nagra.ch/en/downloads/technical-report-ntb-21-03-2/.

Kitamura, A., 2021. JAEA-TDB-RN in 2020: Update of JAEA's Thermodynamic Database for Solubility and Speciation of Radionuclides for Performance Assessment of Geological Disposal of High-Level and TRU Wastes. Japan Atomic Energy Agency. https://jopss.jaea.go.jp/pdfdata/JAEA-Data-Code-2020-020.pdf.

Kraus, K.A., Nelson, F., 1950. Hydrolytic behavior of metal ions. I. The acid constants of uranium(IV) and plutonium (IV). J. Am. Chem. Soc. 72, 3901–3906.

Manfredi, C., Caruso, V., Vasca, E., Vero, S., Ventimiglia, E., Palladino, G., Ferri, D., 2006. On the hydrolysis of the tetravalent uranium ion U4+. J. Solut. Chem. 35, 927–937.

MATLAB, 2022. version R2022a. https://in.mathworks.com/products/new_products/release2022a.html.

Moog, H.C., Bok, F., Marquardt, C.M., Brendler, V., 2015. Disposal of nuclear waste in host rock formations featuring high-saline solutions - Implementation of a thermodynamic reference database (THEREDA). Appl. Geochem. 55, 72–84.

Neck, V., Fanghänel, T., Metz, V., Kienzler, B., 2001. Kenntnisstand zur aquatischen Chemie und der thermodynamischen Datenbasis von Actiniden und Technetium. KIT-INE Report.

Neck, V., Kim, J.I., 2001. Solubility and hydrolysis of tetravalent actinides. Radiochim. Acta 89, 116.

Neck, V., Kim, J.I., Kanellakopulos, B., 1992. Solubility and hydrolysis behaviour of neptunium(V). Radiochim. Acta 56, 25–30.

Opel, K., Weiß, S., Hübener, S., Zänker, H., Bernhard, G., 2007. Study of the solubility of amorphous and crystalline uranium dioxide by combined spectroscopic methods. Radiochim. Acta 95, 143–149.

Parks, G.A., Pohl, D.C., 1988. Hydrothermal solubility of uraninite. Geochem. Cosmochim. Acta 52, 863–875.

Pitzer, K.S., 1991. Activity Coefficients in Electrolyte Solutions. CRC Press.

Pitzer, K.S., 1975. Thermodynamics of electrolytes. V. Effects of higher-order electrostatic terms. J. Solut. Chem. 4, 249–265.

Pitzer, K.S., 1973. Thermodynamics of electrolytes. I. Theoretical basis and general equations. J. Phys. Chem. 77, 268–277.

Pitzer, K.S., Kim, J.J., 1974. Thermodynamics of electrolytes. IV. Activity and osmotic coefficients for mixed electrolytes. J. Am. Chem. Soc. 96, 5701–5707.

Pitzer, K.S., Mayorga, G., 1974. Thermodynamics of electrolytes. III. Activity and osmotic coefficients for 2-2 electrolytes. J. Solut. Chem. 3, 539–546.

Pitzer, K.S., Mayorga, G., 1973. Thermodynamics of electrolytes. II. Activity and osmotic coefficients for strong electrolytes with one or both ions univalent. J. Phys. Chem. 77, 2300–2308.

Plyasunov, A., Fanghänel, T., Grenthe, I., 1998. Estimation of the pitzer equation parameters for aqueous complexes. A case study for uranium at 298.15 K and 1 atm. Acta Chem. Scand. 52, 250–260.

Rai, D., Felmy, A.R., Ryan, J.L., 1990. Uranium(IV) hydrolysis constants and solubility product of UO2·x*H2O(am). Inorg. Chem. 29, 260–264.

Rai, D., Felmy, A.R., Sterner, S.M., Moore, D.A., Mason Batteile, M.J., Novak, C.F., 1997. The solubility of Th(IV) and U(IV) hydrous oxides in concentrated NaCl and MgCU solutions. Radiochim. Acta 79, 239–241.

Rai, D., Yui, M., Moore, D.A., 2003. Solubility and solubility product at 22°C of UO2(c) precipitated from aqueous U(IV) solutions. J. Solut. Chem. 32, 1–17.

Rand, M., Fuger, J., Grenthe, I., Volker, N., Rai, D., 2008. Chemical Thermodynamics of Thorium, Paris. OECD Publishing, Paris. https://www.oecd-nea.org/jcms/pl_14270/chemical-thermodynamics-of-thorium?details=true.

Ryan, J.L., Rai, D., 1983. The solubility of uranium(IV) hydrous oxide in sodium hydroxide solutions under reducing conditions. Polyhedron 2, 947–952.

Tremaine, P.R., Chen, J.D., Wallace, G.J., Boivin, W.A., 1981. Solubility of uranium (IV) oxide in alkaline aqueous solutions to 300°C. J. Solut. Chem. 10, 221–230.

Yajima, T., Kawamura, Y., Ueta, S., 1994. Uranium(IV) solubility and hydrolysis constants under reduced conditions. MRS Online Proc. Libr. 353, 1137.

Yalçıntaş, E., Çevirim-Papaioannou, N., Gaona, X., Fellhauer, D., Neck, V., Altmaier, M., 2019. Solubility of U(VI) in chloride solutions. III. The stable oxides/hydroxides in MgCl2 systems: pitzer activity model for the system UO22+–Na+–K+–Mg2+–H+–OH−–Cl−–H2O(l). J. Chem. Thermodyn. 131, 375–386.